HEAD-TO-TAIL POLYMERIZATION OF MICROTUBULES IN VITRO

Electron Microscope Analysis of Seeded Assembly

LAWRENCE G. BERGEN and GARY G. BORISY

From the Laboratory of Molecular Biology and the Department of Zoology, University of Wisconsin, Madison, Wisconsin 53706

ABSTRACT

Microtubules are polar structures, and this polarity is reflected in their biased directional growth. Following a convention established previously (G. G. Borisy, 1978, *J. Mol. Biol.* **124**:565–570), we define the plus (+) and minus (−) ends of a microtubule as those equivalent in structural orientation to the distal and proximal ends, respectively, of the A subfiber of flagellar outer doublets. Rates of elongation were obtained for both ends using flagellar axonemes as seeds and porcine brain microtubule protein as subunits. Since the two ends of a flagellar seed are distinguishable morphologically, elongation of each end may be analyzed separately. By plotting rates of elongation at various concentrations of subunit protein, we have determined the association and dissociation rate constants for the plus and minus ends. Under our conditions at 30°C, the association constants were 7.2 $\times 10^6$ M^{-1} s^{-1} and 2.25 $\times 10^6$ M^{-1} s^{-1} for the plus and minus ends, respectively, and the dissociation constants were 17 s^{-1} and 7 s^{-1}. From these values and Wegner's equations (1976, *J. Mol. Biol.* **108**:139–150), we identified the plus end of the microtubule as its head and calculated "*s*," the head-to-tail polymerization parameter. Surprisingly small values ($s = 0.07 \pm 0.02$) were found. The validity of models of mitosis based upon head-to-tail polymerization (Margolis et al., 1978, *Nature* (*Lond.*) **272**:450–452) are discussed in light of a small value for *s*.

KEY WORDS microtubule polymerization kinetics · flux

Microtubules possess a structural polarity (2, 6) which is reflected in their directionality of growth (1, 3, 7, 15). Wegner (16) has pointed out that when the formation of a polar linear polymer is chemically coupled to an irreversible exergonic reaction (e.g., the hydrolysis of ATP), the resultant steady state may be characterized by a flux of subunits from one end to the other in which net polymerization at one end (the head) balances net depolymerization at the other (the tail). Wegner referred to this steady-state condition as head-to-tail polymerization. This novel concept is of direct relevance to our understanding of cell division since several models of mitosis (see reference 14 for review) embody the idea of a flux of subunits in spindle fibers, and one recent model (13) is explicitly based on the head-to-tail polymerization mechanism.

Wegner (16) estimated quantitatively the degree

of head-to-tail character for actin polymerization by analyzing the correlation of the kinetics of polymer formation with the exchange of labeled subunits at steady state. The correlation was expressed in terms of the head-to-tail parameter, "s." This parameter can vary between 0 and 1; $s = 0$ signifies bidirectional growth, and $s = 1$ signifies total head-to-tail polymerization, that is, all association events occur at one end, and all of the dissociation events occur at the other end.

For actin polymerization, Wegner determined $s = 0.25$, which means that, on the average, for every four association and four dissociation steps the polymer is lengthened by one subunit at the head, and shortened by one subunit at the tail. Margolis and Wilson (12) studied the exchange of labeled GTP with microtubules at steady state, and estimated a flux (under their conditions) of subunits equivalent to 0.69 μm length of tubule/h. Therefore, microtubules, like actin filaments, show head-to-tail polymerization or, by the terminology of Margolis and Wilson, show opposite end assembly-disassembly. However, Margolis and Wilson did not attempt to correlate their flux rate with the kinetics of microtubule growth, and therefore were not able to calculate the parameter s. Nevertheless, they inferred on the basis of indirect evidence that association and disassociation of subunits from microtubules occur at mutually exclusive sites, a statement equivalent to saying $s \simeq 1$.

It should be emphasized that although the data of Margolis and Wilson pertained to net assembly and disassembly, their conclusions were stated in terms of individual association and dissociation reactions. Some confusion occurs in reading their paper since the words assembly and disassembly were used to signify the separate molecular events as well as the net gain or loss of polymer. Since these distinctions are crucial to this paper, we will use assembly, elongation, and growth interchangeably to signify the net reaction and reserve association for the single bimolecular reaction of a subunit with the end of a tubule, and dissociation for the single unimolecular loss of a subunit from the end of a tubule.

In this paper, we extend Wegner's theory and apply it to the case of seeded assembly of microtubules, using the method of kinetic analysis reported by Johnson and Borisy (11). We use a heterogeneous system consisting of stable flagellar seeds and brain tubulin subunits (1). This permits us to distinguish the two ends of a microtubule from one another and to determine quantitatively the four rate constants that define the polymerization system. Knowledge of the four rate constants permits us to identify which end of a microtubule is its head and to distinguish among several possible patterns of head-to-tail growth. We are able to calculate the magnitude of the steady-state rate of flux and the head-to-tail parameter s, which is a measure of the efficiency of the flux. We find, contrary to the conclusions of Margolis and Wilson (12), that association and dissociation of subunits occur at both ends of a microtubule and that the end possessing the greater rate constant for association also has the greater rate constant for dissociation. From this characterization, we evaluate the validity of mechanisms of mitosis based on head-to-tail polymerization.

MATERIALS AND METHODS

Isolation of Flagella

Flagella were isolated from the unicellular alga *Chlamydomonas reinhardtii* and demembranated according to the procedure of Allen and Borisy (1), with the one modification that the pelleted flagella were resuspended in microtubule polymerization buffer: 100 mM PIPES, 1 mM EGTA, 0.1 mM $MgCl_2$, 1 mM GTP, pH 6.94 (PEMG). Axonemal suspensions were transferred with plastic test tubes and pipettes, since axonemes bound strongly to glass, resulting in poor yields. Axonemes were used in experiments either within 2 h of demembranation or frozen in liquid nitrogen and stored at −80°C. Frozen preparations were stable for at least 2 mo.

The concentration of axonemes was calculated by a method using latex beads as an internal standard. First, the concentration for a solution of small latex beads (0.481 μm Diam, Ernest F. Fullam Inc., Schenectady, N. Y.) was determined with a hemacytometer. Measured volumes of beads and axonemes were then mixed, and the number of each seen in one field (× 400, phase optics, Carl Zeiss Inc., New York) was recorded. From the ratio of beads to axonemes, the concentration of axonemes was calculated. In typical experiments, the final concentration of axonemes was in the range of 8 to 20 × 10^6 axonemes/ml.

Microtubule Protein and Subunit Preparation

Microtubule protein was prepared from porcine brain tissue by two cycles of polymerization and depolymerization with differential centrifugation according to Borisy et al. (5). The buffer used throughout the protein purification, preparation, and experimentation was PEMG. For storage, polymer was collected by centrifugation, frozen in liquid nitrogen, and kept at −80°C. Protein determinations were done as described previously (11).

Non-self-initiating solutions of microtubule protein were prepared by high-speed centrifugation of purified microtubule protein (185,000 g_{avg}; for 90 min, at 4°C). This procedure strongly attenuates the ability of the protein to self-assemble but does not alter the subunit's competence to elongate microtubules (1, 15). The subunit preparations were either used immediately after the high-speed centrifugation or frozen in liquid nitrogen and stored at −80°C without detectable loss of activity. Frozen samples were thawed immediately before use in an experiment.

Electron Microscope and Computer Analysis

Samples were fixed with 2% glutaraldehyde, then applied to 200-mesh grids coated with Formvar and carbon, and stained with 1% uranyl acetate. Electron micrographs were recorded on 70-mm film (Kodak), using a Philips 300 electron microscope. The fixed microtubules were frequently curved, rendering it impractical to determine their lengths with a ruler. For this reason and because a large number of length determinations were required, measurements of lengths were made directly from the projected image of the 70-mm negatives by tracing with a model 264s digitizer (Numonics Corp., Lansdale, Pa.) interfaced with a 9825A computer (Hewlett-Packard Co., Palo Alto., Calif.). After magnification factors were calculated and entered, data were stored as lengths in micrometers of added microtubules at the distal and proximal ends of the flagellar seeds. Data reduction consisted of routinely plotting length histograms and calculating means and standard deviations. The program used was designed originally to trace lengths of DNA molecules for denaturation mapping (9). The program was kindly supplied by Dr. R. Littlewood.

RESULTS

Theory

Our previous kinetic analysis of microtubule elongation (11) showed that the polymerization reaction was characterized by both addition and loss of tubulin dimers at the ends of the microtubule. By analyzing the dependence of elongation rate on subunit concentration, the rate constants for the association (k_2) and dissociation (k_{-1}) reactions were determined. This k_2, however, refers to the sum of the association rate constants for each end ($k_2^+ + k_2^-$); *likewise*, k_{-1} equals $k_{-1}^+ + k_{-1}^-$, where the + and − superscripts denote the plus and minus ends, respectively.

We now seek to determine the rate constants for each end. To accomplish this, we use as seeds flagellar axonemes isolated from the alga, *Chlamydomonas reinhardtii.* As shown previously (1), the ends of the axoneme distal and proximal to the basal body can be distinguished morphologically. Thus, microtubule elongation occurring on the two ends can also be distinguished. Our assumption is that the seed serves as an internal marker of polarity without altering the polymerization kinetics characteristic of the two ends of a microtubule. Net elongation is more rapid on the distal end (1, 3), and we shall refer to it as the plus (+) end, the other end being designated as minus (−). It is important to note here that our designations of plus and minus ends refer to an absolute structural polarity of the microtubule itself. This is operationally distinct from the definition of polymer "head" (16), and "primary assembly site" (12) which refer to the relative net assembly activities of the two ends of a microtubule at steady state. Thus, a priori, our designations predict neither the identity of the plus end as head or tail, nor the direction of steady-state flux.

By rearranging Eq. 1 of Johnson and Borisy (11), it can be shown that the rate of microtubule elongation is given by:

$$cdL/dt = k_2[S] - k_{-1}, \qquad (1)$$

where k_2 and k_{-1} are the rate constants, $[S]$ is the tubulin subunit concentration, and c is a constant of proportionality. This relationship holds true for elongation at both the plus and minus ends, and so can be used to obtain association and dissociation rate constants for each end. Since subunits can contain either GTP or GDP at the exchangeable site, there are, in principle, two species of tubulin to be considered and a total of eight association and disassociation events, each defined by an individual rate constant. Following the reasoning presented by Wegner (16), we assume that the association of GDP-containing subunits is negligible since the reaction is carried out in the presence of excess GTP, and nucleotide exchange is assumed to be rapid. Also, the dissociation of subunits with the concomitant rephosphorylation of GDP to GTP is considered to contribute negligibly to the overall reaction. Therefore, four rate constants (k_2^+ and k_{-1}^+ at the plus end; k_2^- and k_{-1}^- at the minus end), that define reactions as outlined in Fig. 1, are sufficient to describe microtubule polymerization. Thus, the net rate of growth at the plus end is expressed as $k_2^+ [S] - k_{-1}^+$.

By combining Eqs. 10 and 14 of Wegner (16) and converting to our notation, it can be shown that the head-to-tail parameter s is given by:

$$s = k_2^h/(k_2^h + k_2^t) - k_{-1}^h/(k_{-1}^h + k_{-1}^t), \qquad (2)$$

where the h and t superscripts here refer to the head and tail ends respectively. That is, s is the difference at steady state between the proportion of association events at the head (or primary assembly end) of a tubule and the proportion of dissociation events at the same end. Given knowledge of the four rate constants, the end which was the head would be defined by the choice giving positive values of s.

To interpret fully the subsequent kinetic experiments, it is helpful to consider, in advance, possible outcomes. Fig. 2 shows eight possible patterns of growth at the two ends of a protein polymer

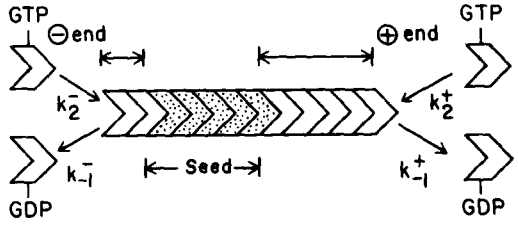

FIGURE 1 Scheme for microtubule polymerization. Assembly and disassembly of microtubule subunits (unstippled chevrons) onto a seed (stippled chevrons) are characterized by two association reactions (k_2^+, k_2^-) and two dissociation reactions (k_{-1}^+, k_{-1}^-). The superscripts, + and −, refer to the plus and minus ends of the microtubule.

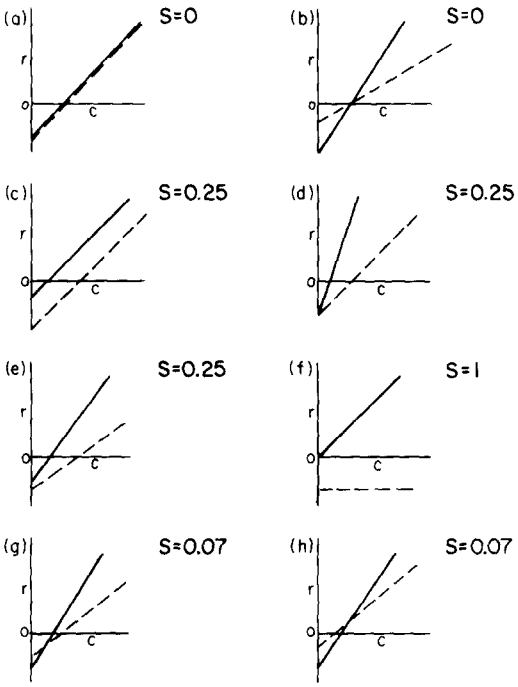

FIGURE 2 Patterns of head-to-tail polymerization. The initial rate of elongation (r) is plotted vs. increasing protein concentration (c) for growth at both the plus end (solid line) and minus end (dotted line) of a microtubule. Values of the head-to-tail polymerization parameter, s, are indicated. See Results for explanation of individual panels.

under the assumption that the kinetics follows Eq. 1. Rates of elongation for both ends are plotted vs. subunit concentration. From the analyses of Johnson and Borisy (11) it has been shown that for such a plot the slopes are proportional to the respective values of k_2, and the intercepts to the values of k_{-1}. Values of s for the individual plots are calculated according to Eq. 2. In most instances the head of the polymer was the end having the greater association constant, but, as will be shown, this was not always the case.

Fig. 2*a* denotes equal bidirectional growth, s equals zero, and no flux occurs. It should be noted, however, that s equals zero for any growth pattern in which the rate plots for both ends intersect at the abscissa (*a* and *b*). Thus, a bias in association of subunits at one end does not necessarily lead to head-to-tail polymerization, since a bias for dissociation at the same end may compensate the difference. The other panels display various possibilities for head-to-tail assembly. The two ends of a linear polymer may have the same association rate constant, but different dissociation constants (*c*); the same dissociation constant but different association constants (*d*); or both the association and dissociation constants may differ (*e–h*). The magnitude of head-to-tail character alone does not fully describe a polymerization system. This is demonstrated by Fig. 2*c*, *d*, and *e* where three possibilities have been drawn such that s equals 0.25. The actin polymerization system (for which $s = 0.25$) (16) may be described by any one of these three panels or by some other set of rate constants yielding the same value of s.

In Fig. 2*e* the end with the greater association rate constant has the lesser dissociation rate, whereas in Fig. 2*g* and *h* the favored end for association is also the favored end for dissociation. In Fig. 2*h* dissociation is so extensively favored at one end that the primary assembly end is the end with the lower association rate constant. This example and Fig. 2*c*, in which the association rate constants are the same for both ends, demonstrate that the end of the tubule with the greater k_2 need not necessarily be the polymerization "head." Fig. 2*f* displays total head-to-tail assembly, that is, association occurs only at one end and dissociation only at the other.

It should be emphasized that neither the subunit exchange data of Wegner (16) nor the flux data of Margolis and Wilson (12) permit one to distinguish among the above possibilities. Our analysis reveals that for an unambiguous identification of the polymerization pattern one requires determination of the four rate constants characterizing the two ends of the microtubule.

Experimental

Microtubule elongation was initiated by mixing solutions of subunits and axonemes. All experi-

ments were done at 30°C in a constant temperature room. Solutions were brought to 30°C before mixing and samples were held in tubes in an aluminum block. At intervals after mixing, 20 μl aliquots were removed and mixed with an equal volume of 2% glutaraldehyde in PEMG to quench the reaction and fix the tubules for subsequent analysis. To calculate rate constants, growth at five concentrations of microtubule subunits was studied. For each concentration, five time points were analyzed. Samples from each of the 25 aliquots were applied to electron microscope grids. From each grid at least 20 microtubules extending proximally and 20 extending distally were measured. When possible, flagella with measurable microtubules on both ends of the axoneme were recorded to minimize error due to local variation. For each flagellum recorded, all microtubules were measured. Altogether, over 1,000 microtubule lengths were measured to construct a single rate plot.

Fig. 3 shows a typical axoneme. The distal end is clearly identifiable as the frayed end, and the length of microtubule extensions on both ends are well defined. The length distribution for proximal and distal tubules were generally pauci-disperse and randomly distributed about the mean. A sample histogram for a set of axonemal microtubules in a polymerization experiment is shown in Fig. 4. All initiation of elongation occurred before 1 min as evidenced by the constant number of elongated microtubules per axoneme throughout the experiment.

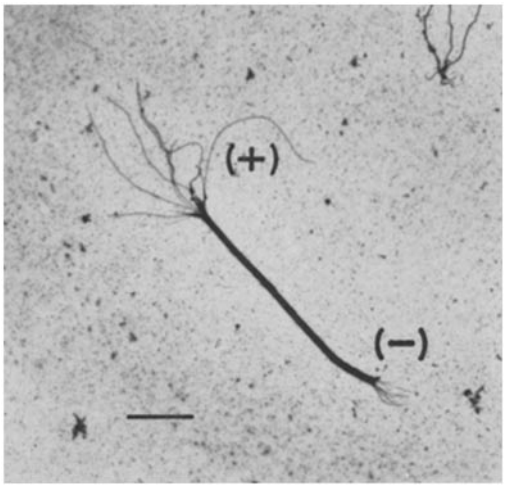

FIGURE 3 Electron micrograph of a typical axoneme with added neurotubules at the distal (+) and proximal (−) ends. This preparation was incubated with 0.7 mg/ml microtubule subunits for 5 min at 30°C. Preparation for electron microscopy was as described in Materials and Methods. Bar, 3 μm.

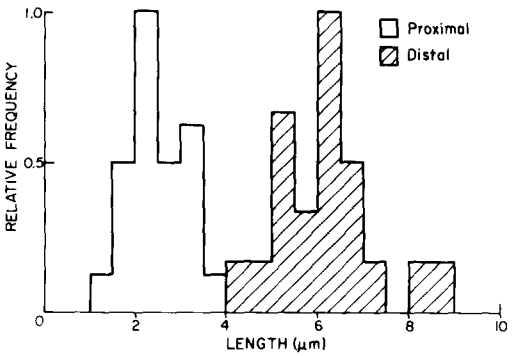

FIGURE 4 Histogram of microtubule lengths for a typical time point of a polymerization experiment. Proximal microtubules (open bars), 23 measured with a mean of 2.5 ± 0.6 μm; distal microtubules (hashed bars), 20 measured with a mean of 6.2 ± 1.1 μm. Incubation time was 3 min with 0.88 mg/ml microtubule subunits at 30°C.

In most cases, growth seeded only by the A subfiber of an outer doublet was observed. However, at higher protein concentration, growth also occurred on the B subfibers. Often it was not possible to distinguish between the growth on the two subfibers. 50 such examples were analyzed by determining the ratio of lengths (shorter/longer) of the two microtubules seeded by one outer doublet. This ratio equaled 0.88 ± 0.09. The closeness of this ratio to a value of 1 indicates that once growth was initiated on the B subfiber, the rates of elongation on both A and B subfibers were equivalent.

The means and standard deviations for the length histograms were plotted against time to yield time-courses of elongation for both proximal and distal ends, such as those shown in Fig. 5. The time points generally fell on straight lines that intersected at the origin. In some experiments the best straight line, as determined by a least squares regression, intersected the abscissa at short times (0–30 s). It is not clear whether these apparent short lags are statistically significant. The slopes of the time-course plots, and the standard deviations of these slopes were then plotted against initial subunit concentrations. This generated a rate plot of the type shown in Fig. 6 and is the cumulative result of ten time-course plots, derived in turn from 50 histograms.

The rate plots for both the plus ends and the minus ends (Fig. 6) were linear, confirming the

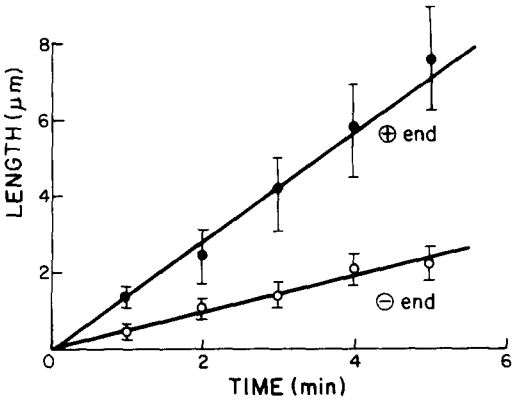

FIGURE 5 Time-course of microtubule elongation. Each point represents the mean and standard deviation of a histogram like that shown in Fig. 4. Protein concentration was 0.66 mg/ml. The rates of elongation were 1.33 ± 0.17 μm/min at the + end (solid circles); 0.45 ± 0.07 μm/min at the − end (open circles).

previous analysis of Johnson and Borisy (11). From the slopes and the intercepts of these plots, rate constants were calculated and are shown in Table I. The values obtained for k_2 are somewhat larger but of the same order of magnitude as those obtained in two previous studies (3, 11). However, the striking and more important result is that the end characterized by the larger association constant (the plus end) is also characterized by the larger dissociation constant. Thus, the pattern of polymerization is of the type shown in Fig. 2*g*. From these values of rate constants and Eq. 2, we identified the plus end as the head or primary assembly end. Furthermore, we calculated the head-to-tail parameter s to be 0.07. The steady-state monomer concentration, $\bar{c}_1$, can be obtained from this plot as the subunit concentration at which positive values of elongation on one end are balanced by negative values at the other. In this experiment $\bar{c}_1$ was found to be 0.3 mg/ml and is located graphically in Fig. 6. The flux can also be determined graphically as the value of elongation at the plus end (or shortening at the minus end) corresponding to the steady-state monomer concentration. Values of steady-state flux obtained from such graphs ranged from 0.034 to 0.076 μm/min.

An s value of 0.07 appeared to be surprisingly low, so we investigated whether it might depend on the particular preparation conditions. Our original experiments used microtubule subunits and axonemes that had been frozen for storage and subsequently thawed. The possibility that the activity of the subunits and/or flagellar seed was altered by freezing and thawing was tested by repeating the experiments with subunits prepared from freshly cycled microtubule protein and with freshly prepared or frozen flagella. In all cases statistically equivalent results were obtained (Table I). We conclude that freezing and thawing does not significantly alter the properties of microtubule protein to elongate tubules nor the ability of the flagellar axoneme to serve as a seed. Since microtubule polymerization is temperature-dependent, the growth experiments were repeated at another temperature (24.5°C; data not shown). At this lower temperature, all four rate constants were reduced but the pattern of growth was similar to that at 30°C.

From Fig. 6 we deduced that the plus end of a microtubule not only has the greater rate constant for association but also the greater rate constant for dissociation. To test this inference we attempted to determine directly the rates of depolymerization. First, microtubules were polymerized onto axonemes as done previously. Then at t = 3 and t = 5 min we removed and fixed aliquots to monitor the rate of polymerization. At t = 5 min 30 s an aliquot (20 μl) was removed and mixed with 200 μl warm (30°C) PEMG. This resulted in

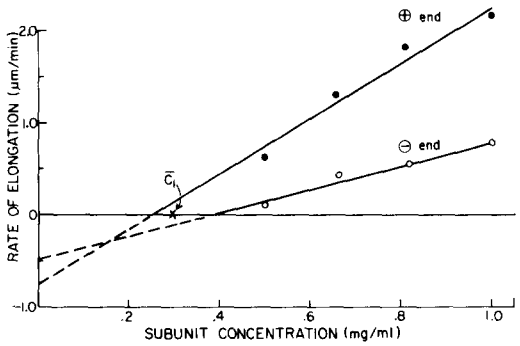

FIGURE 6 Dependence of rate of elongation on subunit concentration. Each point represents the slope of a time-course such as shown in Fig. 5. The data were fit by a least squares linear regression analysis (solid lines) and intercepts on the ordinate were obtained by extrapolation (dotted lines). The slope for growth at the plus end (solid circles) was 3.0 μm/min(mg/ml)$^{-1}$; the intercept was −0.77 μm/min. The slope for the minus end (open circles) was 1.3 μm/min(mg/ml)$^{-1}$; the intercept was −0.48 μm/min. The steady-state monomer concentration ($\bar{c}_1$ = 0.3 mg/ml) is denoted by ×. The correlation coefficients for the plus and minus end lines are 0.97 and 0.98, respectively.

TABLE I

Rate Constants for Association and Dissociation

Condition subunits/seeds	Plus end		Minus end		Head-to-tail parameter
	$k_2^+ \times 10^{-6}\ M^{-1}\ s^{-1}$	$k_{-1}^+\ s^{-1}$	$k_2^- \times 10^{-6}\ M^{-1}\ s^{-1}$	$k_{-1}^-\ s^{-1}$	s
Thawed/thawed	7.2 ± 0.86	16 ± 5	2.2 ± 0.15	7 ± 1	0.07 ± 0.04
Fresh/thawed	6.4 ± 0.30	11 ± 2	2.2 ± 0.26	5 ± 2	0.06 ± 0.03
Fresh/fresh	7.2 ± 0.85	17 ± 6	3.0 ± 0.40	10 ± 3	0.08 ± 0.03

Parameters for microtubule polymerization. Rate constants were calculated for association and dissociation at both (+) and (−) ends under three conditions. Using Eq. 1, values of k_2 were obtained from slopes and values of k_{-1} from ordinates of rate plots such as the one shown in Fig. 5. From these rate constants, the head-to-tail parameter, s, was calculated according to Eq. 2. In the first condition, subunits were prepared as described in Materials and Methods and frozen with liquid nitrogen before use in the experiment. For the latter two conditions, subunits were prepared immediately before the experiment. In the first two conditions the axonemes had been stored frozen, while in the latter case these, too, were prepared immediately before the experiment. Similar values for the association and dissociation rate constants and the head-to-tail parameters were obtained under all three conditions.

an 11-fold dilution of the subunit protein. Since the new subunit concentration was well below the steady-state monomer level, one would expect the microtubules to depolymerize. The amount of depolymerization was expected to be linear initially, and then decrease gradually as a new steady-state plateau was approached. After dilution, aliquots were removed at 30-s intervals, fixed with glutaraldehyde, and prepared for analysis as previously described.

The results, shown in Fig. 7, demonstrate that the predicted kinetic pattern was obtained, and that the depolymerization rate on the distal end was greater than the rate at the proximal end. The rates were 25 subunits/s and 8 subunits/s for the plus and minus ends, respectively. These values are rates of depolymerization at monomer concentration approaching zero and may be compared to the corresponding values, derived by extrapolation from the growth experiments. Agreement is good, although the plus end depolymerized somewhat faster than predicted. The important point however, is that the experiment provides direct evidence that the rate constant for dissociation is greater at the so-called primary assembly end (equivalent to the head) than at the primary disassembly end (equivalent to the tail).

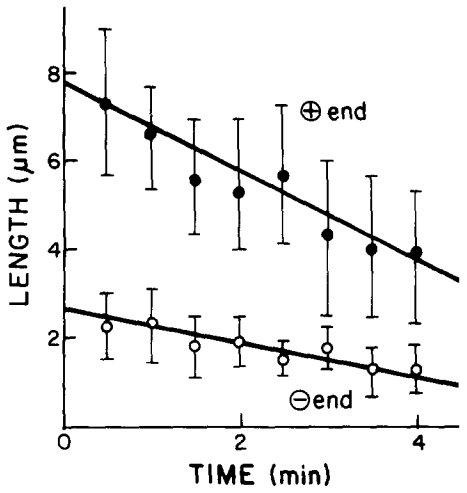

FIGURE 7 Time-course of dilution-induced depolymerization. Microtubules were polymerized onto axonemes as described previously. After growth had proceeded to an extent of 6–9 μm on the plus end and 2–3 μm on the minus end, an aliquot was removed and diluted 11-fold with buffer at 30°C, reducing the protein concentration to 0.06 mg/ml. This is noted as time zero. Then, at intervals of 30 s, aliquots were removed and fixed to monitor depolymerization. Rates of depolymerization were 0.98 ± 0.10 μm/min for the plus end (solid circles), 0.30 ± 0.06 μm/min for the minus end (open circles). The correlation coefficient for the plus and minus end lines are −0.96 and −0.88, respectively.

DISCUSSION

In this study we have used a heterogeneous system of flagellar seeds and brain microtubule subunits to determine the rate constants for addition of subunits at the two ends of a cytoplasmic microtubule. This analysis rests on the assumption that the growth properties of the added microtubules are indistinguishable from those of cytoplasmic microtubules. Once the flagellar tubules have been extended with brain subunits, subsequent subunits will see an environment of brain subunits at the growing end. We would argue that these later subunits should not be able to distinguish between binding to a microtubule initiated by a flagellar

seed or a free microtubule. This seed activity is intrinsic to the flagellar tubules since no matter where the flagella are broken, the ends are competent to serve as seeds. Furthermore, we assume that the added tubule and the flagellar seed are continuous at their union; that is, in a physical sense there is no "end" at the point of union, and neither addition nor loss of subunits occurs at the join. Thus, the only sites available for addition and loss of subunits are the ends of the added tubules on either side of the flagellar seed. The stable flagellar seed serves to separate the two ends of the labile cytoplasmic microtubules and make them available for independent analysis.

Another assumption of the analysis is that the time-course of polymerization is linear under the conditions that we analyze. We would expect a linear time-course only if the monomer concentration did not change appreciably during the time assayed. This assumption was tested by calculating the total amount of polymer formed and comparing that value with the initial monomer concentration. The extent of polymer formation was estimated from the number concentration of flagella (see Materials and Methods), the average number of microtubules per flagellum, the greatest length of microtubules attained in the experiments, and the number of tubulin subunits (1,625) per micrometer of tubule. From these figures we calculated that no more than 0.1% of the monomer was converted to polymer during any experiment, thus changes in monomer concentration were negligible, and a linear time-course was to be expected.

Our analysis confirms qualitatively the existence of head-to-tail polymerization in microtubules as reported by Margolis and Wilson (12). It goes further in identifying the plus end of the microtubule, the end equivalent to the distal end of flagellar tubules, as the head. This is the first determination of the direction of flux relative to the absolute structural orientation of a microtubule. Our analysis also determines all four rate constants, specifies the pattern of head-to-tail growth, namely, the pattern shown in Fig. 2 *g*, and determines the magnitude of the head-to-tail parameter, *s*, under our conditions to be 0.07.

We wish to note that the value of *s* has so far been determined only under a given set of conditions. Perhaps under other conditions a different value of *s* will be found. An interesting possibility to explore is that the value of *s* might be modulated by cellular regulatory mechanisms.

The flux may be calculated from the steady-state monomer concentration and the rate constants as:

$$\text{flux} = k_2^+ \bar{c}_1 - k_{-1}^+ = -(k_2^- \bar{c}_1 - k_{-1}^-). \quad (3)$$

The steady-state monomer concentration was obtained from plots such as Fig. 6 after correcting for the proportion of total protein which was nontubulin (20%) and the proportion of tubulin subunits which was active (80%). Rate constants were taken from Table I. The flux was calculated to be 0.056 ± 0.020 μm/min, in agreement with the values determined graphically. The steady-state flux corresponds to a net flow through the tubule of two dimers per second. This rate is five times the value of 0.69 μm/h reported by Margolis and Wilson (12). The reason for the difference in results is not known; however, different methods, conditions, and materials were used in the two studies.

To avoid confusion, it might be helpful to relate further our results to those of Margolis and Wilson (12). Those authors concluded that "the microtubule assembly-disassembly 'equilibrium' is a steady-state summation of two different reactions which occur at opposite ends of the microtubule, and that assembly and disassembly occur predominantly and perhaps exclusively at the opposite ends under steady-state conditions *in vitro*." It is clear that the authors are referring to separate sites for association and dissociation, and suggesting that little or no dissociation occurs at the head and similarly little or no association occurs at the tail. In contrast, our results show that association and dissociation occur to a significant degree at both ends of a microtubule. Indeed, the rate constant for association is greater at the head than at the tail of the microtubule, but the dissociation constant is also greater at the head than the tail. Nevertheless, the proportion of total dissociation steps occurring at the plus end is less than the proportion of association steps at that end, so that a flux results from the plus to the minus end.

The discrepancy between our conclusions and those of Margolis and Wilson are not easily accounted for by minor differences in solution conditions. The discrepancy seems to arise from the fact that they measured net addition or loss of subunits from polymer, whereas we have dissected the net reactions into an algebraic sum of addition and loss at each end.

Our results may be significant for models of mitosis based on assembly-disassembly (10, 8) and in particular a recent model by Margolis et al. (13)

which is predicated on the head-to-tail polymerization mechanism. Their model "envisages a constant assembly of microtubules at the equatorial region of the spindle and at the kinetochores coupled with a poleward migration of subunits within the microtubules as they flow towards the disassembling ends." Microtubule assembly in kinetochore-to-pole fibers occurs proximal to the kinetochore. At anaphase, assembly at the kinetochore is blocked, resulting in net disassembly of these microtubules and the poleward movement of sister chromatids.

The head-to-tail parameter, s, can be taken as a measure of the efficiency of the flux. A value of $s = 1$ signifies that every subunit added at one end or lost at the other contributes directly to the flux. A value of s equal to or approaching 1 seems to be implicit in the model of Margolis et al. (13) and in the conclusions of the earlier paper by Margolis and Wilson (12).

However, our determination of the head-to-tail parameter indicates that, at least under our in vitro conditions, the flux is an inefficient process. We have determined $s = 0.07$. This indicates that 14 association steps and 14 dissociation steps on the average lead to a lengthening of the microtubule by one subunit at the growing end (head) and to a shortening by one subunit at the degrading end (tail) at steady state. From the rate constants, we calculate that the net lengthening of a tubule by one subunit at its head involves the addition of 11 and loss of 10 subunits, and the shortening by one subunit at the tail involves the addition of three and loss of four subunits. Thus, both ends of a microtubule display a level of dynamic activity not previously considered.

Also, our result that both ends of a microtubule can add and lose subunits does not fit well with the idea of Margolis et al. (13) that in anaphase the head is blocked allowing the tail end to disassemble. Assuming their premise and our results to be valid, then the tail would still be free to add and lose subunits. Net loss of subunits would occur transiently, but the net loss would cease when the tubules came to a steady-state balance with a new, higher concentration of monomer.

Head-to-tail polymerization is such a novel and intriguing concept that one is disposed to assume that if it exists, it must be put to good biological purpose. But, if the degree of head-to-tail character is so slight ($s = 0.07$), and if we cannot make a strong case for its role in mitosis, then what significance can we attach to the phenomenon?

It seems to us that the question is whether microtubules have been designed to flux subunits from one end to the other, or whether this property is incidental to some other aspect of tubule polymerization. Wegner (16) has shown that head-to-tail polymerization is dependent upon an irreversible energy-yielding step, which for actin is the hydrolysis of ATP. For microtubules the corresponding step is the hydrolysis of GTP, however, the function of nucleotide binding and hydrolysis has yet to be established. Perhaps indeed the role of GTP is to allow head-to-tail polymerization when at steady state. Alternatively, the GTP may serve some other purpose such as facilitating the independent control of microtubule formation and breakdown. Although this view is not mutually exclusive with fluxing, it suggests that head-to-tail assembly may be an incidental consequence of tubulin-GTP interactions and hydrolysis. These questions cannot be answered on the basis of the available data.

We thank Dr. R. Littlewood for his assistance with the computer programming, and Dr. R. H. Rownd for the use of the computer facilities. We also thank Drs. R. B. Scheele and C. Allen as well as Mr. R. Cote for critically reading this manuscript.

This study was supported by National Institutes of Health (NIH) grant GM 25062 to G. G. Borisy. L. G. Bergen was supported by an NIH predoctoral traineeship.

Received for publication 25 June 1979, and in revised form 10 August 1979.

REFERENCES

1. ALLEN, C., and G. G. BORISY. 1974. Structural polarity and directional growth of microtubules of *Chlamydomonas* flagella. *J. Mol. Biol.* **90:** 381–402.
2. AMOS, L., and A. KLUG. 1974. Arrangement of subunits in flagellar microtubules. *J. Cell Sci.* **14:**523–549.
3. BINDER, L., W. DENTLER, and J. L. ROSENBAUM. 1975. Assembly of chick brain tubulin onto flagellar microtubules from *Chlamydomonas* and sea urchin sperm. *Proc. Natl. Acad. Sci. U. S. A.* **72:**1122–1126.
4. BORISY, G. G. 1978. Polarity of microtubules of the mitotic spindle. *J. Mol. Biol.* **124:**565–570.
5. BORISY, G. G., J. M. MARCUM, J. B. OLMSTED, D. B. MURPHY, and K. A. JOHNSON. 1975. Purification of tubulin and associated high molecular weight proteins from porcine brain and characterization of microtubule assembly *in vitro*. *Ann. N. Y. Acad. Sci.* **253:**107–132.
6. CREPEAU, R., B. MCEWEN, G. DYKES, and S. EDELSTEIN. 1977. Structural studies on porcine brain tubulin in extended sheets. *J. Mol. Biol.* **116:**301–315.
7. DENTLER, W., S. GRANETT, G. B. WITMAN, and J. L. ROSENBAUM. 1974. Directionality of brain microtubule assembly in vitro. *Proc. Natl. Acad. Sci. U. S. A.* **71:**1710–1714.
8. DIETZ, R. 1972. Assembly hypothesis of chromosome movement. *Chromosoma (Berl.).* **38:**11–76.
9. INMAN, R. B. 1967. Some factors affecting electron microscopic length of deoxyribonucleic acid. *J. Mol. Biol.* **25:**209–216.
10. INOUÉ, S. 1964. Organization and function of the mitotic spindle. *In* Primative Motile Systems in Cell Biology. R. D. Allen and N. Kamiya, editors. Academic Press, Inc., New York.

11. JOHNSON, K. A., and G. G. BORISY. 1977. Kinetic analysis of microtubule assembly *in vitro*. *J. Mol. Biol.* **117**:1–31.
12. MARGOLIS, R. L., and L. WILSON. 1978. Opposite end assembly and disassembly of microtubules at steady state *in vitro*. *Cell* **13**:1–8.
13. MARGOLIS, R. L., L. WILSON, and B. KIEFER. 1978. Mitotic mechanism based on intrinsic microtubule behavior. *Nature* (*Lond.*). **272**:450–452.
14. NICKLAS, R. B. 1977. Chromosome movement: Facts and hypotheses. *In* Mitosis Facts and Questions. Little, Paweletz, Petzelt, Ponstingl, Schroeter, Zimmermann, editors. Springer-Verlag, Berlin.
15. OLMSTED, J. B., J. M. MARCUM, K. A. JOHNSON, C. ALLEN, and G. G. BORISY. 1974. Microtubule assembly: some possible regulatory mechanisms. *J. Supramol. Struct.* **2**:429–450.
16. WEGNER, A. 1976. Head to tail polymerization of actin. *J. Mol. Biol.* **108**:139–150.